Comparative Biochemistry and Physiology, Part C 250 (2021) 109174

Contents lists available at ScienceDirect

Comparative Biochemistry and Physiology, Part C

journal homepage: www.elsevier.com/locate/cbpc

Ferritin H can counteract inflammatory response in hybrid fish and its parental species after *Aeromonas hydrophila* infection

Ning-Xia Xiong [a], Sheng-Wei Luo [a,*], Zhuang-Wen Mao [b], Lan-Fen Fan [c], Kai-Kun Luo [a], Shi Wang [a], Fang-Zhou Hu [a], Ming Wen [a], Qing-Feng Liu [a], Shao-Jun Liu [a,*]

[a] State Key Laboratory of Developmental Biology of Freshwater Fish, College of Life Science, Hunan Normal University, Changsha 410081, PR China
[b] Hunan Provincial Key Laboratory of Nutrition and Quality Control of Aquatic Animals, Department of Biological and Environmental Engineering, Changsha University, Changsha 410022, PR China
[c] College of Marine Sciences, South China Agricultural University, Guangzhou 510642, PR China

ARTICLE INFO

Edited by Martin Grosell

Keywords:
Hybrid fish
Ferritin H
Innate immunity
Inflammation

ABSTRACT

Ferritin H can participate in the regulation of fish immunity. Tissue-specific analysis revealed that the highest expressions of Ferritin H in parental species were observed in spleen, while peaked level of Ferritin H mRNA in hybrid fish was observed in liver. In addition, *A. hydrophila* challenge could sharply enhance their Ferritin H mRNA expression in liver, kidney and spleen. To further investigate their roles in immune regulation, their Ferritin H fusion proteins were produced *in vitro*. Ferritin H fusion proteins could exhibit a direct binding activity to *A. hydrophila* and endotoxin in a dose-dependent manner, restrict dissemination of *A. hydrophila* to tissues and abrogate inflammatory cascades. Moreover, treatment with Ferritin H fusion proteins could reduce *A. hydrophila*-induced lipid peroxidation. These results indicated that Ferritin H in hybrid fish elicited a similar immune regulation of *A. hydrophila*-induced inflammatory signals in comparison with those of its parents.

1. Introduction

Environmental pollution can pose a great risk to public health and lead to the occurrences of severe diseases (Qi et al., 2020). In general, ambient stressors may alter physiological response and elicit an immunosuppressive effect in fish (Magnadottir, 2010). Although iron is an essential nutrient that can serve as a critical component of cytochromes, oxygen-binding molecules and enzymes (Andrews, 1999), excessive level of intracellular iron can damage cellular macromolecules and promote cell death which is largely due to its ability to catalyze the generation of radicals (Papanikolaou and Pantopoulos, 2005). Increased studies have demonstrated that iron can establish pro-oxidant status and mediate oxidative damage, showing a mutual dependence between iron homeostasis and oxidative stress (Meneghini, 1997). Evidences are emerging that Ferritin can also serve as acute phase protein (APP), participating in immune defense against pathogenic infection, occurrences of malignancies and autoimmune diseases (Beard et al., 2006; Ong et al., 2005; Zandman-Goddard and Shoenfeld, 2007).

In general, fish contain various forms of pathogen-recognizing properties as well as developed complement cascades and apoptosis-related signals (Holland and Lambris, 2002; Luo and Wei, 2020). Among known APPs, Ferritin is a major iron-regulating protein consisting of Ferritin H and Ferritin L in mammals (Worwood, 1990), while Ferritin H and Ferritin M are the predominant subunits in fish (Scudiero et al., 2013). Although most studies focus on function of mammalian APP genes synchronizing innate immunity with adaptive immune response, only a few reports study on the architecture and expression of Ferritin H in teleost, such as salmon (Andersen et al., 1995), channel catfish (Liu et al., 2010), large yellow croaker (Zhang et al., 2010) and blunt snout bream (Ding et al., 2017). In our previous studies, Ferritin H in hybrid fish and its parents could mitigate the inflammatory signals in respective fish cell lines (Luo et al., 2021a), but the data on comparative analysis of immune defense against bacterial invasion of Ferritin H in hybrid fish and its parents are sparse.

Hybridization is a predominant evolutionary event that gives rise to species with novel capabilities. Meanwhile, chimeric genes may form through fusion of pieces of various genomes (Rogers et al., 2009), and then change gene structures and alter signal transductions upon *in vitro* stimuli (Koyama et al., 2007; Liu et al., 2016). Recent studies reveal that hybrid offspring can exhibit a strong resistance against pathogenic

* Corresponding authors at: College of Life Science, Hunan Normal University, Changsha 410081, PR China.
E-mail addresses: swluo@hunnu.edu.cn (S.-W. Luo), lsj@hunnu.edu.cn (S.-J. Liu).

https://doi.org/10.1016/j.cbpc.2021.109174
Received 6 June 2021; Received in revised form 6 August 2021; Accepted 22 August 2021
Available online 28 August 2021

infection in comparison with those of its parental species (Šimková et al., 2013; Šimková et al., 2015). Crucian carp (*Carassius auratus*) is one of the most important economic freshwater fish and abundant in lakes, rivers and reservoirs in China, which is popular with fish farmers (Li et al., 2018). Currently, white crucian carp (*Carassius cuvieri*, WCC) and red crucian carp (*Carassius auratus* red var, RCC) are classified into different species in the genus of *Carassius* (J. Luo et al., 2014), thus generation of hybrid crucian carp (WR) by crossing of WCC (2n = 100, ♀) and RCC (2n = 100, ♂) is considered as interspecific hybridization (Liu et al., 2019). Apart from documented problems, aquaculture of crucian carp is ravaged from environmental deterioration, which may render fish less resistant to pathogenic infection (Bowden, 2008; Choo et al., 2018). Additionally, the emergence of global climate change may exhibit a lingering effect in the expansion of water-borne pathogenic diseases, posing an increased threat to the survival of aquatic organisms (Marcogliese, 2008). Previous studies demonstrate that *A. hydrophila* challenge can significantly increase accumulative mortality of allogynogenetic crucian carp (Liu et al., 2013). Thus, this study on comparative analysis of immune response to *A. hydrophila* infection in hybrid crucian carp and its parents may be propitious to the sustainable development of aquaculture.

In this study, the aims were to compare the tissue distribution of RCC/WCC/WR-Ferritin H mRNA and measure their expression patterns after *A. hydrophila* challenge. To further characterize their function, we studied *in vitro* binding activity of RCC/WCC/WR-Ferritin H to *A. hydrophila* and lipopolysaccharide (LPS). In addition, we investigated their immunoregulatory effect on bacterial dissemination *in vivo* and inflammatory response, which may provide a new insight to the immune regulation of hybrid fish.

2. Materials and methods

2.1. Ethics approval

All applicable international, national, and/or institutional guidelines for the care and use of animals were followed. We followed the laboratory animal guideline for the ethical review of the animal welfare of China (GB/T 35892–2018).

2.2. Preparation of experimental animals

According to previous studies, diploid hybrid fish (WR) was generated by crossing white crucian carp (*Carassius cuvieri*, WCC, ♀) and red crucian carp (*Carassius auratus* red var, RCC, ♂) (Liu et al., 2018; Wang et al., 2015). RCCs, WCCs and WRs were obtained from an aquaculture base in Wang Cheng district (Changsha, Hunan province, China). RCCs, WCCs and WRs were acclimatized in 70 × 65 × 65 cm plastic aquarium (25 fishes/aquarium) with the diluted freshwater (pH 8.0, 23 ± 1 °C) for two weeks. RCCs, WCCs and WRs were fed with commercial diet twice daily till 24 h before challenge experiment. In addition, water quality was properly controlled to avoid pathogenic contamination during fish acclimation or immune challenge.

2.3. Immune challenge with A. hydrophila and fish sampling

Based on our previous studies, *A. hydrophila* strain was cultured for 24 h at 28 °C, centrifuged at 10,000 ×*g* for 15 min at 4 °C, and resuspended in 1 × PBS (pH 7.3). The concentration of *A. hydrophila* was adjusted to 1×10^7 CFU ml^{-1} before the immune challenge experiment (Luo et al., 2020a). RCCs, WCCs and WRs (average length 15.6 ± 0.82 cm) were intraperitoneally injected with 100 μl suspension of 1×10^7 CFU ml^{-1} *A. hydrophila* in PBS, while RCCs, WCCs and WRs injected with 100 μl sterile PBS were used as the control group (Van Doan et al., 2013). PBS treatment and *A. hydrophila* treatment of RCCs, WCCs and WRs contained three replicates under the same conditions, respectively. The individuals were anesthetized with 100 mg/L MS-222 (Sigma-Aldrich, St Louis, MO, USA) to minimize suffering prior to sampling. Tissues were isolated at 0, 6, 12, 24, 36 and 48 h post-injection, immediately frozen in liquid nitrogen and preserved in −80 °C.

2.4. Quantitative real-time PCR (qRT-PCR) assay

2.4.1. RNA isolation and cDNA synthesis

Total RNA isolation and cDNA synthesis were performed as previously described (Luo et al., 2021b). Total RNA was extracted from isolated tissues by using HiPure Total RNA Mini kit (Magen, China). Then, concentration and integrity of purified total RNA were determined by measurement of 260/280 nm absorbance and agarose gel electrophoresis, respectively (Luo et al., 2015a). 1000 ng of purified total RNA was used for cDNA synthesis using Revert Aid™ M-MuLV Reverse Transcriptase Kit (MBI Fermentas, USA).

2.4.2. Expression profiles of Ferritin H mRNA determined by qRT-PCR assay

Tissue-specific and *A. hydrophila*-stimulated expression patterns of RCC-Ferritin H, WCC-Ferritin H and WR-ferritin H were examined by using Applied Biosystems QuantStudio 5 Real-Time PCR System (Applied Biosystems, USA). qRT-PCR assay contained 1 cycle of 95 °C for 30 s, 40 cycles of 95 °C for 15 s, 60 °C for 35 s, followed by 1 cycle of 95 °C for 30 s, 60 °C for 60 s. At the end of qRT-PCR amplified reactions, melting curve analysis was implemented to confirm credibility of each qRT-PCR analysis (Qi et al., 2013). Besides, the expression of 18S rRNA (XR_003291850.1) was measured and used as internal control to normalize results of qRT-PCR analyses (Luo et al., 2016). Primer specificity was confirmed and each sample was analyzed in triplicate. The primers were shown in Table 1. qRT-PCR results were measured with $2^{-\Delta\Delta Ct}$ methods (Livak and Schmittgen, 2001).

2.5. Plasmid preparation

Open reading frame (ORF) sequence of RCC-Ferritin H, WCC-Ferritin H and WR-Ferritin H were obtained in our previous studies (Luo et al., 2021a). To further investigate their immune function, the above ORF sequences were ligated to pET32a plasmid and transformed into *Escherichia coli* DH5α complement cells. The positive single bacterial clone was selected and cultured in Luria-Bertani (LB) liquid medium containing 100 μg/ml ampicillin. Finally, obtained bacterial clones were sequenced by Tsingke Biotechnology Co., Ltd. (Beijing, China).

2.6. Production of Ferritin H fusion proteins

2.6.1. Prokaryotic expression and purification

Fusion proteins were produced by prokaryotic expression system as previously described (Luo et al., 2019a). In brief, pET32a, pET32a-RCC-Ferritin H, pET32a-WCC-Ferritin H and pET32a-WR-ferritin H plasmid were transformed into *E. coli* BL21 (DE3) competent cells, respectively. BL21 clones inserted with corrected plasmids were cultured in LB medium with 100 μg/ml ampicillin at 37 °C until OD600 value reached about 0.6 and continued to incubate with 1 mM isopropyl-β-D-thiogalactopyranoside (IPTG) for another 4 h. After IPTG induction and sonication, pellets were harvested, dissolved in the buffer containing 8 M urea and centrifuged, then the soluble recombinant proteins were obtained and purified by using Ni-NTA resins (Novagen, China).

2.6.2. Western blotting of Ferritin H fusion proteins

Based on previous studies, western blotting was performed (Luo et al., 2017). Purified proteins were loaded on 12% SDS-PAGE gel, separated electrophoretically and washed in TBST buffer. After that, the separated proteins were transferred to Bio-Rad PVDF membranes on ice at 100 V for 90 min by using a western blotting system (Bio-Rad, USA). The membranes were washed in Tris buffered saline with tween 20 (TBST) for 5 min, incubated with blocking buffer containing 3% BSA for

Table 1
The primer sequences used in this study.

Primer names	Sequence direction (5′ → 3′)	Use
pET-*Eco*RI-FerH-F	CCGGAATTCATGTCGGAACCGAGAGTAAA	Vector
pET-Xhol-FerH-R	CCGCTCGAGTTAATGATGATGATGATGATGAGTGATTGTCAGTGTGTCTT	Vector
RT-18S-F	CCGACCCTCCCTCACG	qPCR
RT-18S-R	GCCTGCTGCCTTCCTTG	qPCR
RT-FerH-F	GAGGCAAAACTTCCCGACTG	qPCR
RT-FerH-R	CCACTGGGCAAGCACGAG	qPCR
RT-TIRAP-F	AGCAGCATTGGAAAATACTTGG	qPCR
RT-TIRAP-R	TCGGTGTTGGATTCGTTGATA	qPCR
RT-MyD88-F	CTATGAGGCGATTCCAGTAACA	qPCR
RT- MyD88-R	CCAGTCTGCTGCCACCG	qPCR
RT-TRAF6-F	AGACCAGCAAGGCTATGACG	qPCR
RT- TRAF6-R	GCCGAGCGAAGACCCA	qPCR
RT-IL-1β-1-F	CCTGACAGTGCTGGCTTTG	qPCR
RT- IL-1β-1-R	AATGATGATGTTCACCACCTTC	qPCR
RT-IL-1β-2-F	TCTTCGCATCCTCACAGCAT	qPCR
RT-IL-1β-2-R	CAGCGTCACAGCCTTCAAAT	qPCR
RT-TNFα-1-F	GGATTGCTGCCCTCACGG	qPCR
RT-TNFα-1-R	CTTTGGACACTTTAGGTTCATACG	qPCR
RT-TNFα-2-F	GTGGGGTCCTGCTGGCT	qPCR
RT-TNFα-2-R	CTGGTCCTGGTTCTGTTTC	qPCR
RT-hlyA-F	GGCCGGTGGCCCGAAGATACGGG	qPCR
RT-hlyA-R	GGCGGCGCCGGACGAGACGGGG	qPCR
RT-GAPDH-F	CAGGGTGGTGCCAAGCG	qPCR
RT-GAPDH-R	GGGGAGCCAAGCAGTTAGTG	qPCR

2 h and then incubated with 1:2000 diluted His-tag antibody at 4 °C overnight. Following wash with TBST buffer, membranes were incubated with 1:2000 diluted peroxidase-conjugated antibody for 60 min at room temperature. PVDF membranes were developed and visualized. Following dialysis, the protein concentration was determined by Bradford method (Cha et al., 2015).

2.7. Enzyme linked immunosorbent assay (ELISA) assay

Based on previous studies, 96-well plates were coated with resuspension of *A. hydrophila* (1×10^7 CFU ml^{-1}) or LPS (100 μg/ml, purified from *Escherichia coli* O111:B4, Sigma, USA) at 4 °C overnight, then blocked with 5% milk and washed with 0.5% Tween-20/PBS (Luo et al., 2020b). After that, various concentrations of purified pET32a tag or WR-ferritin H were added to the plates for 2 h incubation at room temperature, followed by incubation with anti-His antibody and horseradish peroxidase (HRP) secondary antibody. Then, 200 μl of tetramethylbenzidine (TMB) diluted in substrate buffer was added and incubated for 30 min in dark. Until the color was developed, 2 M H_2SO_4 was added. The absorbance at 450 nm was determined by a microplate reader. pET32a tag group was served as the control. The experiment was performed in triplicate. The binding index was calculated as described previously (Luo et al., 2019b).

2.8. In vivo effect of Ferritin H fusion proteins on A. hydrophila infection

To investigate the effect of RCC-Ferritin H, WCC-Ferritin H and WR-Ferritin H on growth of *A. hydrophila*, *in vivo* injection was performed as described previously (Wang et al., 2017). Thirty minutes after bacterial infection (1×10^7 CFU ml^{-1}), RCCs, WCCs and WRs received intraperitoneal injection of purified pET32a tag, RCC-Ferritin H, WCC-Ferritin H and WR-Ferritin H at a dose of 4.0 μg/g, respectively. Then, both genomic DNA of tissues and bacterial DNA were extracted by using a DNA extraction kit (Omega, USA), and the concentration was adjusted to 100 ng/μl. qRT-PCR assay was used to detect haemolysin (hlyA, JF738032.1) of *A. hydrophila*, while GAPDH was analyzed as the reference gene. pET32a tag-treated group was used as the control. The experiments were performed in triplicate.

2.9. Protective effect of Ferritin H fusion proteins on inflammatory response following A. hydrophila infection

To investigate the effect of RCC-Ferritin H, WCC-Ferritin H and WR-Ferritin H on inflammatory response following *A. hydrophila* infection, above fusion protein treated samples were used for RNA isolation and cDNA synthesis. Then, qRT-PCR assay was performed as described above (Luo et al., 2020c). pET32a tag treated group was used as the control. The primers of Toll-interleukin 1 receptor domain containing adaptor protein (TIRAP, MG659314.1), myeloid differentiation factor 88 (MyD88, KC816578.1), TNF receptor-associated factor 6 (TRAF6, KF767099.1), Interleukin-1β-1 (IL-1β-1, KC306642.1), Interleukin-1β-2 (IL-1β-2, KC771268.1), tumor necrosis factor α-1 (TNFα-1, KJ923252.1), tumor necrosis factor α-2 (TNFα-2, KJ923253.1) and 18S rRNA were shown in Table.1. Each sample was analyzed in triplicate to certify the repetitiveness and credibility of experimental results. qRT-PCR results were measured by using Applied Biosystems QuantStudio 5 Real-Time PCR System (Applied Biosystems, USA) with $2^{-\Delta\Delta Ct}$ methods.

2.10. Measurement of total superoxide dismutase (SOD) activity

Based on the previous studies, the above fusion protein treated liver samples were homogenized and their protein concentrations were quantified by bicinchoninic acid (BCA) method (Luo et al., 2015b). According to the protocol of total SOD activity kit (Beyotime Biotechnology, Shanghai, China), the enzymatic activities in supernatants of above homogenates were measured as the changes in absorbance at 560 nm by using a Synergy 2 multi-detection microplate reader (Bio-Tek, USA) (Luo et al., 2015c). The results of this enzymatic assay were given in units of SOD activity per milligram of protein, where 1 U of SOD is defined as the amount of enzyme producing 50% inhibition of SOD. The results were repeated in triplicate.

2.11. Measurement of catalase (CAT) activity

CAT activity was measured by ammonium molybdate spectrophotometric method (Yu et al., 2008). According to protocol of catalase (CAT) activity kit (Nanjing Jiancheng Bioengineering Institute, Nanjing, China), the reaction compounds could be monitored by the absorbance at 405 nm. The results of enzymatic assay were given in units of CAT

activity per milligram of protein, where 1 U of CAT is defined as the amount of enzyme decomposing 1 μmol H_2O_2 per second. The results were repeated in triplicate.

2.12. Determination of malondialdehyde (MDA) production

Free MDA and lipid hydroperoxides can be selected determined by thiobarbituric acid (TBA) method (Schmedes and Hølmer, 1989). According to protocol of lipid peroxidation MDA assay kit (Beyotime Biotechnology, Shanghai, China), MDA amount in supernatants of above homogenates were measured by using a Synergy 2 multi-detection microplate reader (Bio-Tek, USA) (S.-W. Luo et al., 2014). The concentration of MDA was expressed as nanomole MDA per milligram protein. The results were repeated in triplicate.

2.13. Statistical analyses

The data analysis was measured by using SPSS 18 analysis program and represented as means ± standard deviation. All of the experimental data analysis was subjected to Student's *t*-test or one-way ANOVA (one-way analysis of variance). In the further analysis of Duncan's multiple range test, only if the level of P-value < 0.05, the differences were considered statistically significant.

3. Results

3.1. Gene expression profiles of RCC-Ferritin H, WCC-Ferritin H and WR-Ferritin H mRNA

In Fig. 1A–C, tissue-specific RCC-Ferritin H, WCC-Ferritin H and WR-Ferritin H mRNA expression were observed in all isolated tissues (L: liver; I: intestine; K: kidney; G: gill; M: muscle; B: brain; S: spleen). High-level mRNA expressions of RCC-Ferritin H and WCC-Ferritin H were observed in spleen, whereas the highest expression level of WR-Ferritin H mRNA was observed in liver.

Moreover, expression profiles of RCC-Ferritin H, WCC-Ferritin H and WR-Ferritin H in liver, kidney and spleen were investigated at 0, 6, 12, 24, 36 and 48 h after *A. hydrophila* challenge. As shown in Fig. 2A–C, the dramatic fluctuation of liver RCC-Ferritin H expression was detected after *A. hydrophila* challenge and reached the peaked level at 48 h, while expression levels of RCC-Ferritin H mRNA in kidney and spleen peaked at 12 h post-infection. In Fig. 2D–F, the highest expressions of WCC-Ferritin H mRNA in liver and kidney were observed at 48 h post-infection, while splenic Ferritin H mRNA expression peaked at 24 h following *A. hydrophila* challenge, followed by a sharp decrease from 36 h to 48 h. Fig. 2G–I, expression levels of WR-Ferritin H mRNA in liver, kidney and spleen began to increase at 6 h and peaked at 36 h, 6 h and 12 h, respectively.

3.2. Prokaryotic expression and fusion protein validation

pET32a-RCC-Ferritin H, pET32a-WCC-Ferritin H, pET32a-WR-Ferritin H and pET32a plasmid were transformed into *E. coli* BL21 (DE3) competent cells for protein expression, respectively. After IPTG induction, whole cell lysates were detected by SDS-PAGE. In. Fig. 3A–C, fusion protein bands were visualized in pET32a-RCC-ferritin H, pET32a-WCC-ferritin H, pET32a-WR-ferritin H transformed cells compared with that of pET32a transformed cells, respectively. Following sonication, RCC-Ferritin H, WCC-Ferritin H and WR-Ferritin H fusion proteins were purified by using a Ni-NTA resin (Millipore), and then confirmed by western blotting using anti-His antibody.

3.3. Binding activity of RCC-Ferritin H, WCC-Ferritin H and WR-Ferritin H to A. hydrophila and LPS

In Fig. 4A–B, RCC-Ferritin H, WCC-Ferritin H and WR-Ferritin H

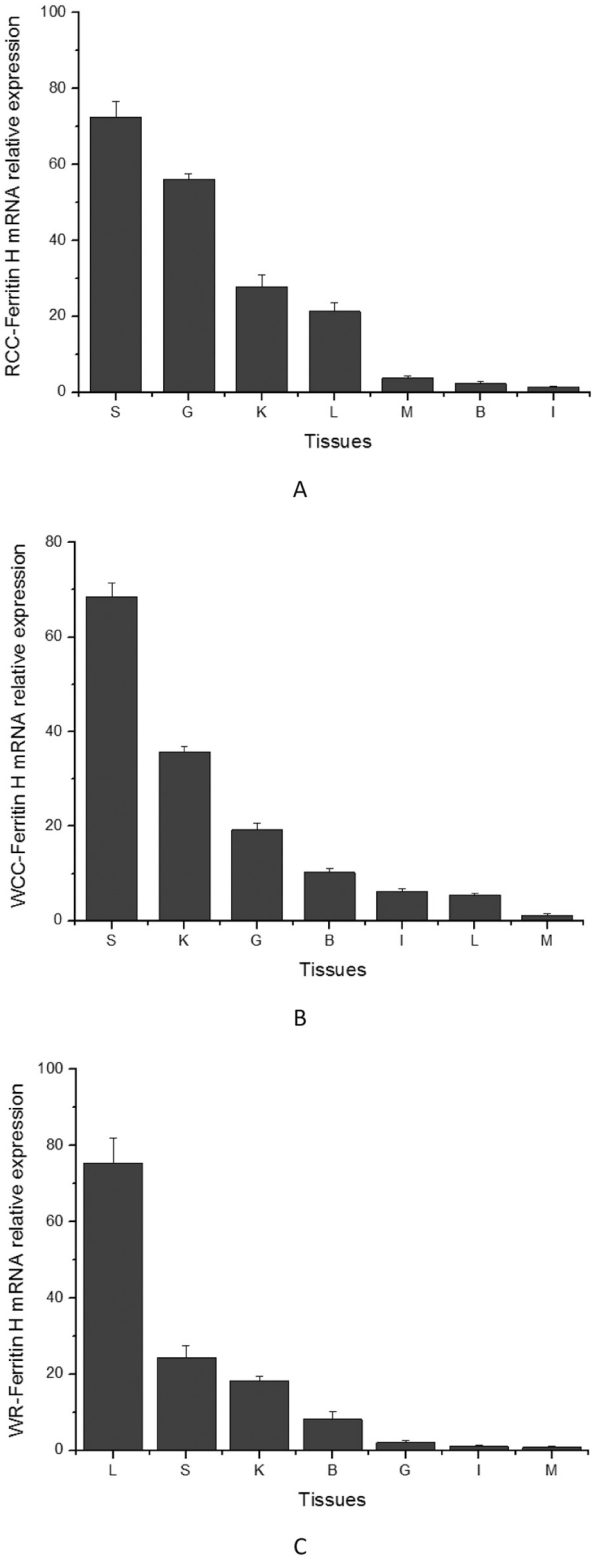

Fig. 1. Tissue-specific expressions of RCC-Ferritin H, WCC-Ferritin H and WR-Ferritin H mRNA.
Relative RCC-Ferritin H (A), WCC-Ferritin H (B) and WR-Ferritin H (C) mRNA expression of each tissue was calculated by the $2^{-\Delta\Delta Ct}$ methods using 18S rRNA as a reference gene, and the relative mRNA level was compared with spleen expression. (L: liver; I: intestine; K: kidney; G: gill; M: muscle; B: brain; S: spleen.)

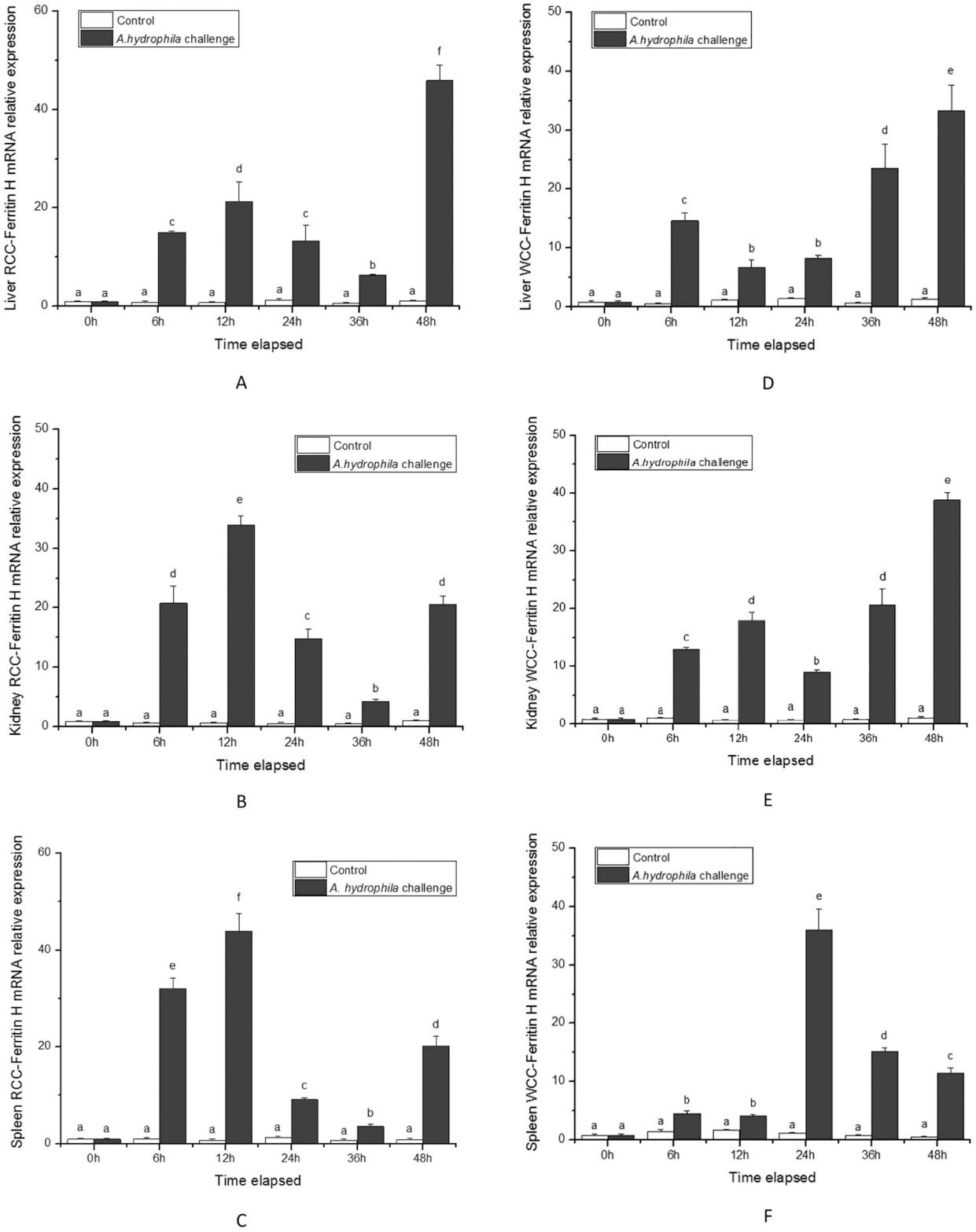

Fig. 2. qRT-PCR analysis of RCC-Ferritin H (A–C), WCC-Ferritin H (D–F) and WR-Ferritin H (G–I) mRNA expression in liver, kidney and spleen at 0, 6, 12, 24, 36 and 48 h post-challenge. The calculated data (mean ± SD) of six individuals (n = 6) with different letters were significantly different ($P < 0.05$).

fusion proteins exhibited a gradual increase of *in vitro* binding ability to *A. hydrophila* and LPS in comparison with those of the control, suggesting that RCC-Ferritin H, WCC-Ferritin H and WR-Ferritin H could elicit a direct binding to *A. hydrophila* and LPS in a dose-dependent manner.

3.4. *In vivo inhibitory effect of RCC-Ferritin H, WCC-Ferritin H and WR-Ferritin H on the growth of A. hydrophila*

In Fig. 5A, expressions of *A. hydrophila* hlyA in liver, kidney and spleen in *A. hydrophila* + RCC-Ferritin H group were approximately

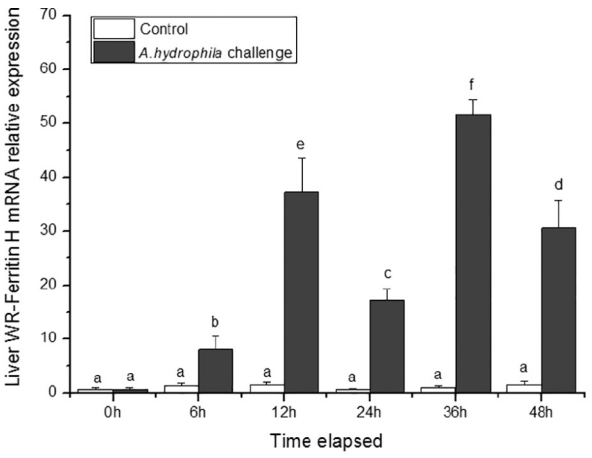

G

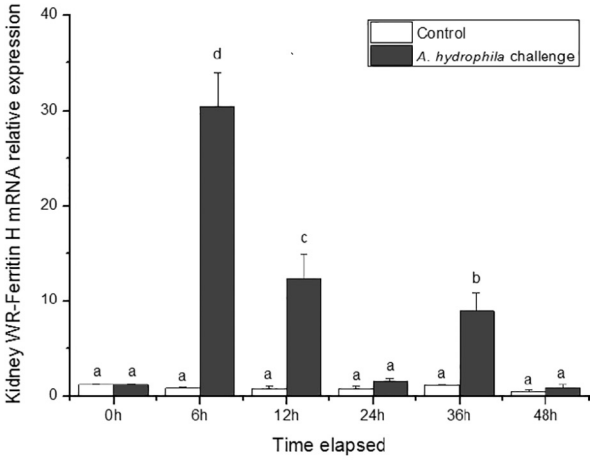

H

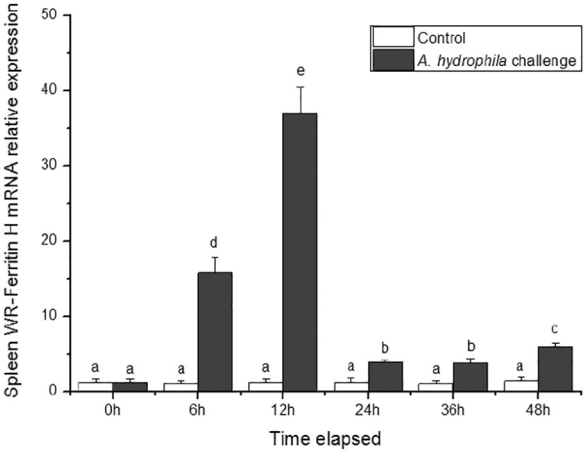

I

Fig. 2. (*continued*).

6.75-, 5.81- and 2.83-fold lower than those of *A. hydrophila* + pET32α tag group, respectively. In Fig. 5B, expressions of *A. hydrophila* hlyA in liver, kidney and spleen showed a 4.96-, 10.94- and 2.56-fold decrease in *A. hydrophila* + WCC-Ferritin H group, respectively. In Fig. 5C, a 4.95-, 12.86- and 10.59-fold decrease of *A. hydrophila* hlyA expression in liver, kidney and spleen was observed in *A. hydrophila* + WR-Ferritin H group. These results suggested that the administration of RCC-Ferritin H, WCC-Ferritin H and WR-Ferritin H can mitigate *in vivo* dissemination of *A. hydrophila* to tissues.

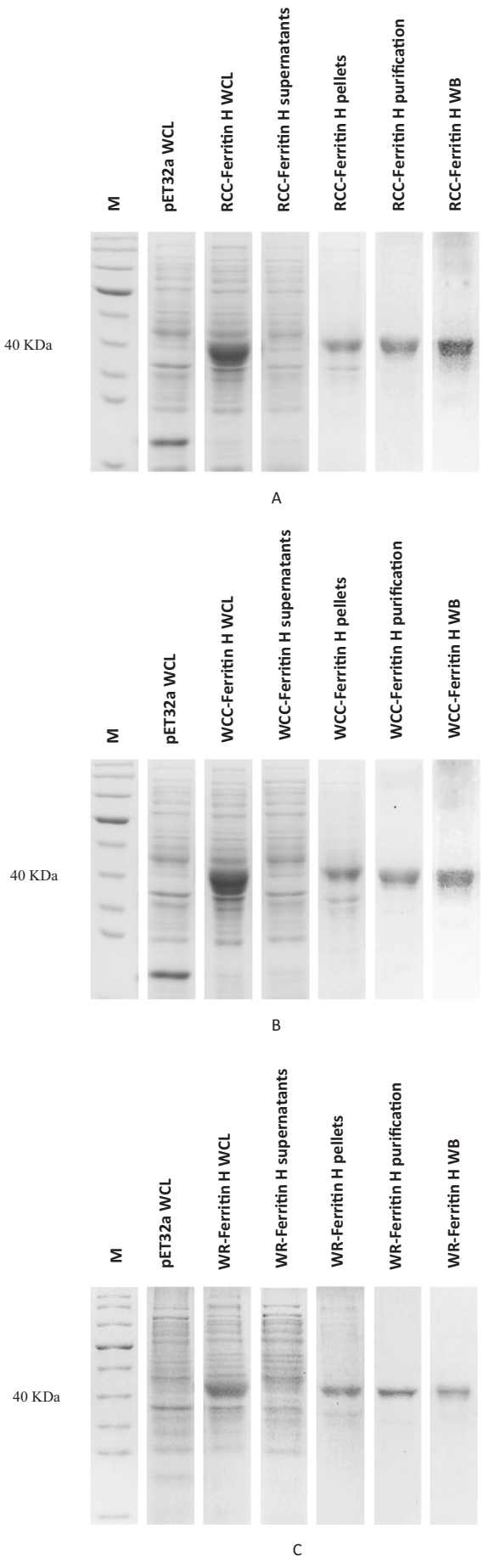

Fig. 3. Generation and purification of RCC-Ferritin H, WCC-Ferritin H and WR-Ferritin H fusion protein. Lane M: Protein molecular standard; Lane pET32a WCL: Total protein was isolated from IPTG induced pET32a-BL21; Lane RCC/WCC/WR-Ferritin H WCL: Total protein was isolated from whole cell lysis of IPTG induced pET32a-RCC/WCC/WR-Ferritin H-BL21; Lane RCC/WCC/WR-Ferritin H supernatants: Supernatants isolated from IPTG induced pET32a-RCC/WCC/WR-Ferritin H-BL21 after sonication; Lane RCC/WCC/WR-Ferritin H pellets: Pellets isolated from IPTG induced pET32a-RCC/WCC/WR-Ferritin H-BL21 after sonication; Lane RCC/WCC/WR-Ferritin H purification: Purified RCC/WCC/WR-Ferritin H fusion protein; Lane RCC/WCC/WR-Ferritin H WB: Purified RCC/WCC/WR-Ferritin H fusion protein was identified by western blotting using anti-His tag antibody.

3.5. Regulatory effect of RCC-Ferritin H, WCC-Ferritin H and WR-Ferritin H on A. hydrophila-stimulated inflammatory cascades

To investigate the immunoregulatory effect of RCC-Ferritin H, WCC-Ferritin H and WR-ferritin H on *A. hydrophila*-induced inflammatory signal molecules (Fig. 6) and cytokine expressions (Fig. 7), transcript levels of TIRAP, MyD88, TRAF6, IL-1β-1, IL-1β-2, TNFα-1 and TNFα-2 were detected at 24 h post-challenge.

In RCCs, liver expression levels of TIRAP, MyD88, TRAF6, IL-1β-1, IL-1β-2, TNFα-1 and TNFα-2 showed a 2.35-, 12.34-, 15.10-, 2.47-, 13.71-, 42.28- and 1.84-fold decrease in *A. hydrophila* + RCC-Ferritin H group, respectively. In kidney, expression levels of TIRAP, MyD88, TRAF6, IL-1β-1, IL-1β-2, TNFα-1 and TNFα-2 in *A. hydrophila* + RCC-Ferritin H group were approximately 5.93-, 5.48-, 5.86-, 3.56-, 2.57-, 15.86- and 3.20-fold lower than those of the control, respectively. In addition, a 3.77-, 12,36-, 11.79-, 2.51-, 3.95-, 25.32- and 6.46-fold decrease of TIRAP, MyD88, TRAF6, IL-1β-1, IL-1β-2, TNFα-1 and TNFα-2 expression was observed in *A. hydrophila* + RCC-Ferritin H group, respectively.

In WCCs, liver expression levels of TIRAP, MyD88, TRAF6, IL-1β-1, IL-1β-2, TNFα-1 and TNFα-2 in *A. hydrophila* + WCC-Ferritin H group were approximately 8.07-, 2.25-, 4.54-, 2.56-, 1.56-, 18.45- and 4.41-fold lower than those of the control, respectively. In kidney, TIRAP, MyD88, TRAF6, IL-1β-1, IL-1β-2, TNFα-1 and TNFα-2 expression levels exhibited a 3.41-, 54.46-, 2.21-, 10.32-, 3.17-, 1.56- and 1.91-fold decrease in *A. hydrophila* + WCC-Ferritin H group, respectively. In addition, splenic expression levels of TIRAP, MyD88, TRAF6, IL-1β-1, IL-1β-2, TNFα-1 and TNFα-2 in *A. hydrophila* + WCC-Ferritin H group were approximately 18.11-, 10.59-, 42.05-, 4.60-, 3.24-, 7.33- and 1.32-fold lower than those of the control, respectively.

In WRs, liver expression levels of TIRAP, MyD88, TRAF6, IL-1β-1, IL-1β-2, TNFα-1 and TNFα-2 in *A. hydrophila* + WR-Ferritin H group were about 3.06-, 13.50-, 31.82-, 5.95-, 13.23-, 16.01- and 14.09-fold lower than those of the control, respectively. Kidney expressions of TIRAP, MyD88, TRAF6, IL-1β-1, IL-1β-2, TNFα-1 and TNFα-2 in *A. hydrophila* + WR-Ferritin H group showed a 9.90-, 4.95-, 36.07-, 6.39-, 18.33-, 51.02- and 12.79-fold decrease by comparing with those of the control, respectively. In addition, a 3.71-, 5.42-, 56.67-, 4.13-, 1.98-, 19.40- and 10.29-fold decrease in the expressions of TIRAP, MyD88, TRAF6, IL-1β-1, IL-1β-2, TNFα-1 and TNFα-2 in *A. hydrophila* + WR-Ferritin H group was detected in comparison with those of the control, respectively.

3.6. Effect of RCC-Ferritin H, WCC-Ferritin H and WR-Ferritin H on A. hydrophila-induced oxidative stress

To investigate antioxidant function of RCC-Ferritin H, WCC-Ferritin H and WR-ferritin H on *A. hydrophila* infection, total SOD activity, MDA amount and CAT activity in liver were detected at 24 h post-infection. As shown in Fig. 8, a sharp increase of total SOD activity and CAT activity in liver were observed in RCC/WCC/WR-Ferritin H treated group at 24 h post-infection by comparing with those of the control, respectively. In contrast, fish receiving the *in vivo* administration of RCC/WCC/WR-Ferritin H exhibited a reduced MDA amount in liver in comparison

(caption on next column)

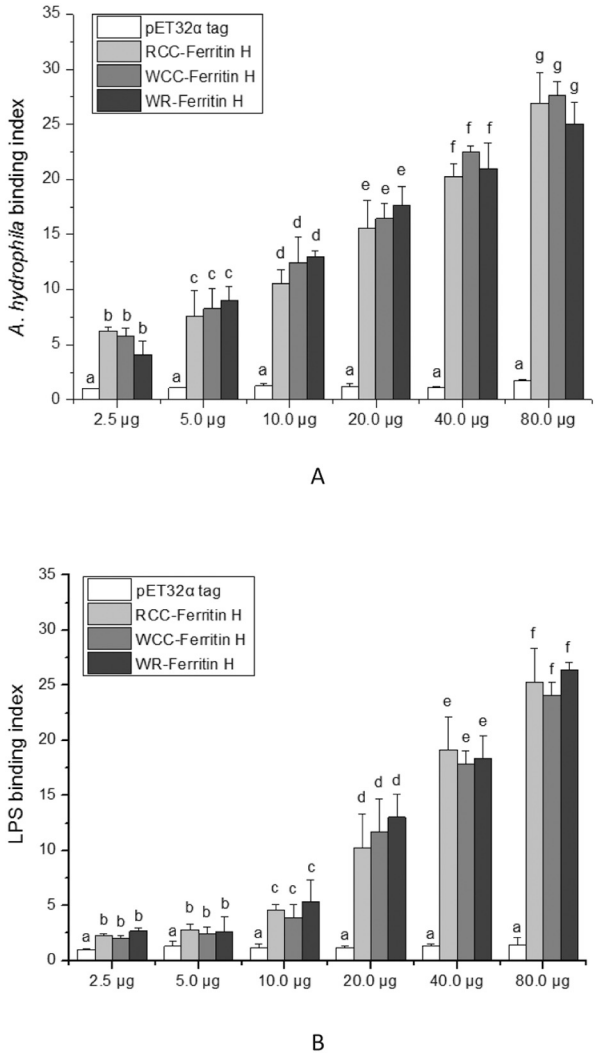

Fig. 4. Binding activity of RCC-Ferritin H, WCC-Ferritin H and WR-Ferritin H fusion protein to *A. hydrophila* (A) and LPS (B) determined by ELISA assay. The calculated data (mean ± SD) with different letters were significantly different ($P < 0.05$) among the groups. The experiments were performed in triplicate.

with those of the control, respectively.

4. Discussion

Ferritin H is a ubiquitous iron-binding protein of ferritin-like superfamily, possessing a ferritin-like domain and seven conserved metal binding sites. In this study, RCC-Ferritin H, WCC-Ferritin H and WR-Ferritin H mRNA were expressed a wide range of isolated tissues, which is similar to previous studies (Ding et al., 2017). In addition, the highest expression levels of RCC-Ferritin H and WCC-Ferritin H was observed in spleen, while a strong expression of WR-Ferritin H mRNA was observed in liver.

Previous studies have demonstrated that kidney and spleen are the major lymphoid tissues, whose populations of lymphocytes and macrophages are capable of mounting an immune response (Press and Evensen, 1999). In addition, Liver can increase the synthesis and secretion of acute phase proteins (APPs) in response to tissue trauma or infection, which may function in limiting the dispersal of infectious agents, repairing tissue damage as well as killing potential pathogens (Bayne and Gerwick, 2001). In this study, RCCs, WCCs and WRs receiving *A. hydrophila* infection exhibited the elevated expressions of RCC-Ferritin H, WCC-Ferritin H and WR-Ferritin H in liver, kidney and

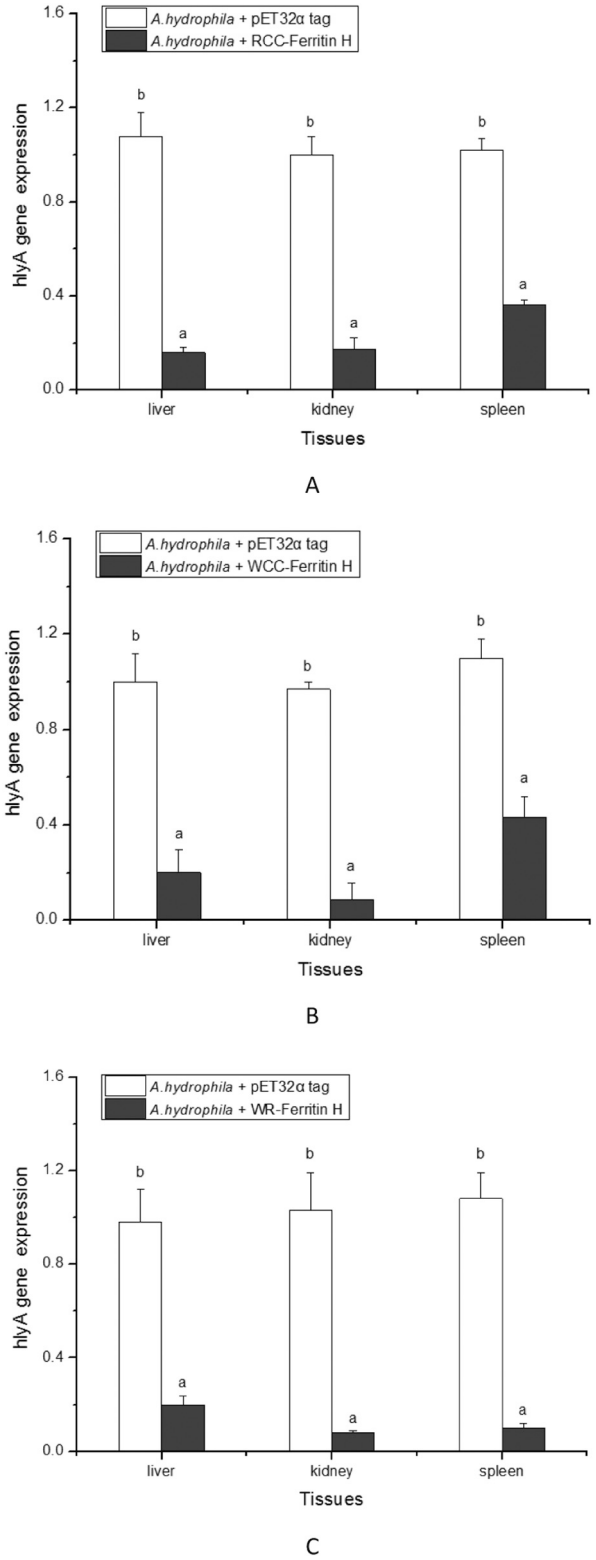

Fig. 5. *In vivo* inhibitory effect of RCC-Ferritin H, WCC-Ferritin H and WR-Ferritin H fusion protein on *A. hydrophila* infection. Expression of *A. hydrophila* hlyA gene was determined by qPCR assay. The calculated data (mean ± SD) with different letters were significantly different ($P < 0.05$) among the groups. The experiments were performed in triplicate.

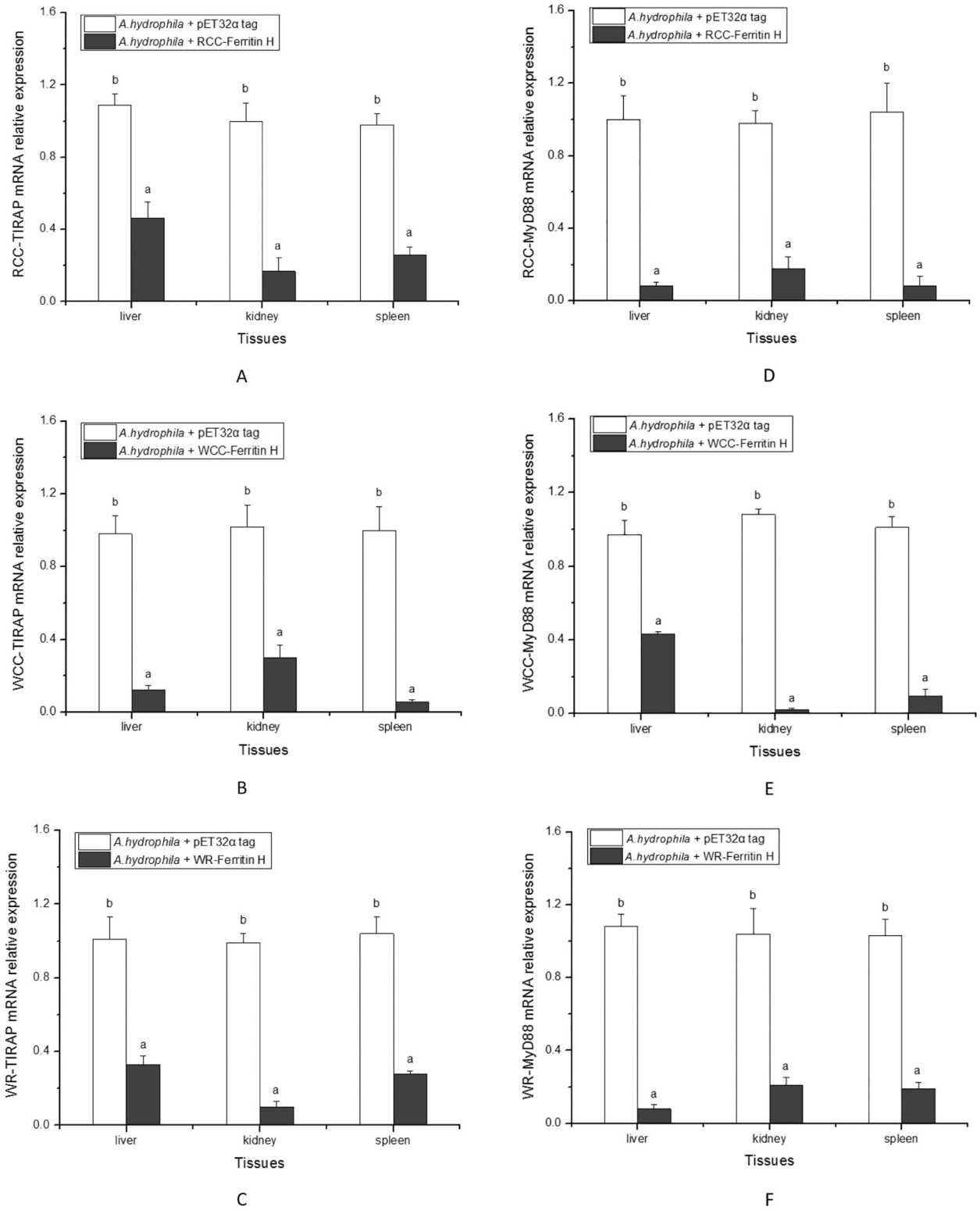

Fig. 6. Immunoregulatory effect of RCC-Ferritin H, WCC-Ferritin H and WR-Ferritin H fusion protein on *A. hydrophila*-induced inflammatory cascades. qRT-PCR analysis of TIRAP (A–C), MyD88 (D–F) and TRAF6 (G–I) mRNA expression in liver, kidney and spleen at 24 h post-challenge. The calculated data (mean ± SD) with different letters were significantly different ($P < 0.05$) among the groups. The experiments were performed in triplicate.

spleen, respectively. These studies implied that RCC-Ferritin H, WCC-Ferritin H and WR-Ferritin H may be involved in immune response to *A. hydrophila* infection. In our previous study, Ferritin H in hybrid offspring and its parents can exhibit a similar downregulatory effect in LPS induced nuclear factor-κB (NF-κB) inflammatory signal in fish cells (Luo et al., 2021a). However, comparative mechanism on *in vivo* inhibitory effect of Ferritin H on *A. hydrophila*-induced inflammatory response in hybrid offspring and its parents was not clear.

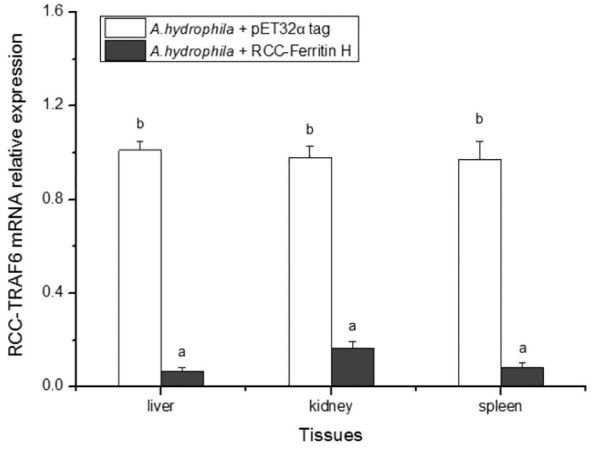

G

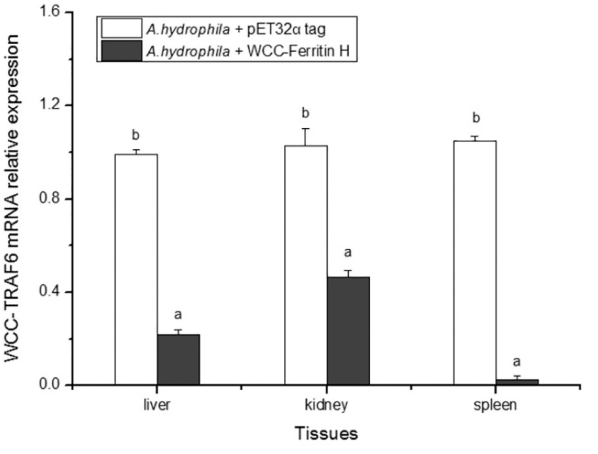

H

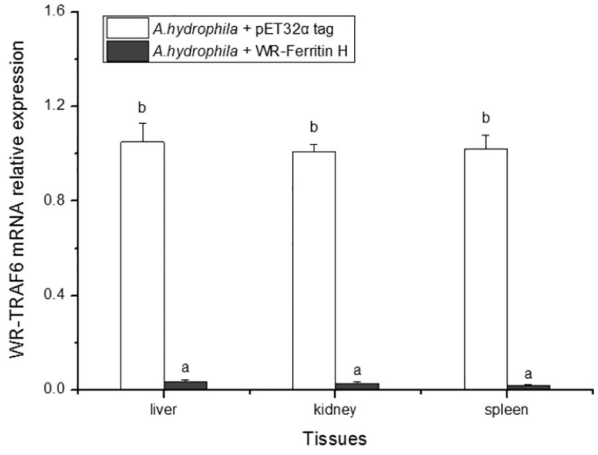

I

Fig. 6. (*continued*).

To elucidate the mechanism linking Ferritin H to immune regulation between hybrid offspring and its parents, RCC-Ferritin H, WCC-Ferritin H and WR-Ferritin H recombinant proteins were produced. Then, ELISA assay revealed that RCC-Ferritin H, WCC-Ferritin H and WR-Ferritin H could exhibit a direct binding activity to *A. hydrophila* and LPS in a dose-dependent manner. Additionally, *in vivo* administration of RCC-Ferritin H, WCC-Ferritin H and WR-Ferritin H could diminish the expressions of *A. hydrophila* hlyA in liver, kidney and spleen, suggesting that Ferritin H derived from hybrid offspring and its parents can alleviate bacterial disseminations to tissues *in vivo*.

A. hydrophila is a gram-negative bacteria, posing an increasing threat to the survival of economic fish (Gonzalez-Serrano et al., 2010).

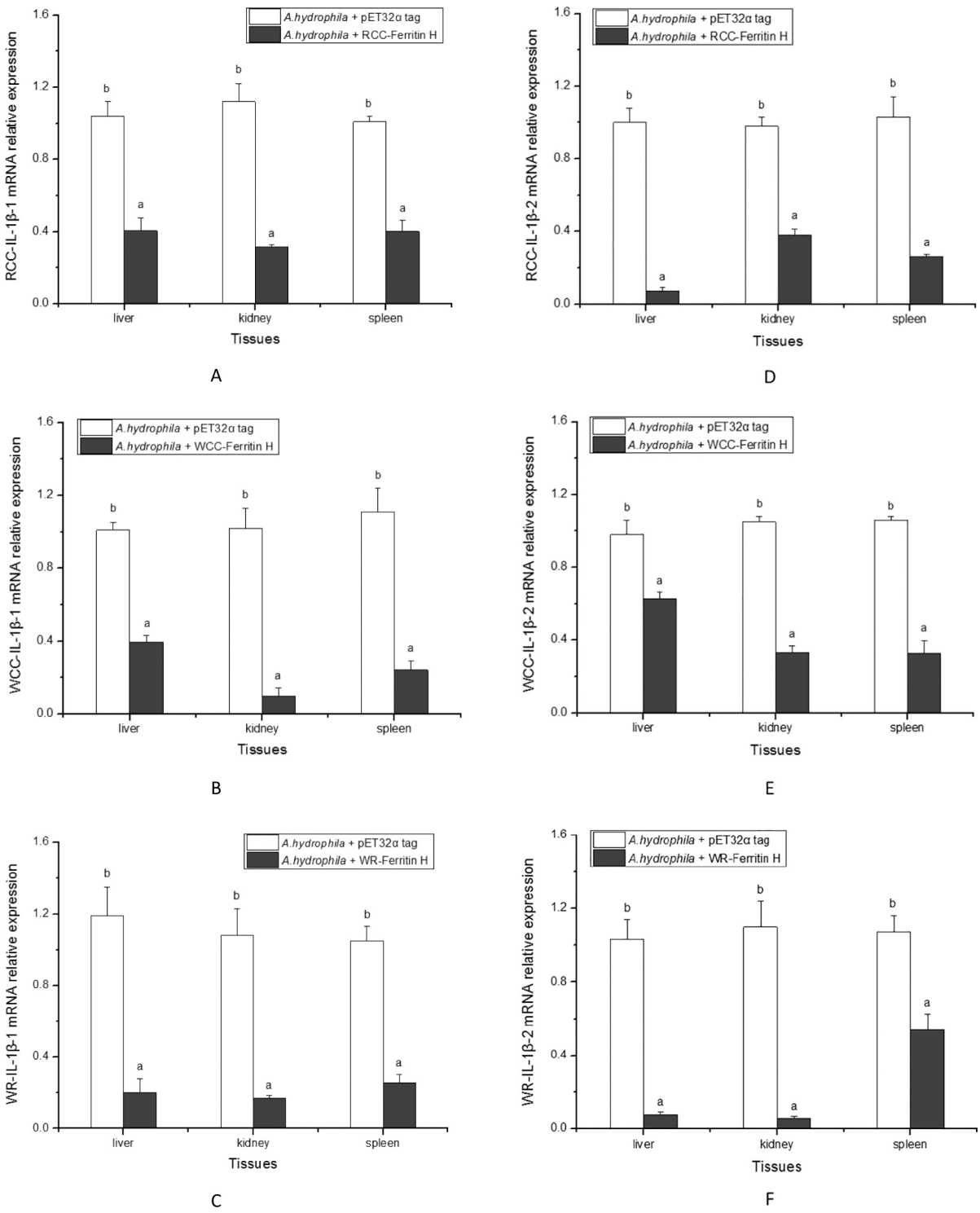

Fig. 7. Immunoregulatory effect of RCC-Ferritin H, WCC-Ferritin H and WR-Ferritin H fusion protein on *A. hydrophila*-induced cytokine expressions. qRT-PCR analysis of IL-1β-1 (A–C), IL-1β-2 (D–F), TNFα-1 (G–I) and TNFα-2 (J–L) mRNA expression in liver, kidney and spleen at 24 h post-challenge. The calculated data (mean ± SD) with different letters were significantly different ($P < 0.05$) among the groups. The experiments were performed in triplicate.

Furthermore, LPS is an endotoxin on the outer membrane of gram-negative bacteria, which is involved in innate and adaptive immunity through Toll-like receptor (TLR) signals (Triantafilou et al., 2004). Toll-interleukin 1 receptor domain containing adaptor protein (TIRAP) serves as a major adaptor involved in the connection of LPS-activated TLR signals (Horng et al., 2002), then triggering the recruitment of myeloid differentiation factor 88 (MyD88) (Kawai et al., 1999). The TNF receptor-associated factor 6 (TRAF6) is a critical signal molecule participating in induction of MyD88-induced NF-κB activation (Muroi and Tanamoto, 2008). As is well known, NF-κB is a key transcription factor capable of determining the choice between life or death events (Karin and Lin, 2002), participating in cytokine production (Diomede et al., 2017; Hunter and De Plaen, 2014) and apoptotic regulation (Wang et al., 1996; Zhu et al., 2011). Current studies revealed that expression

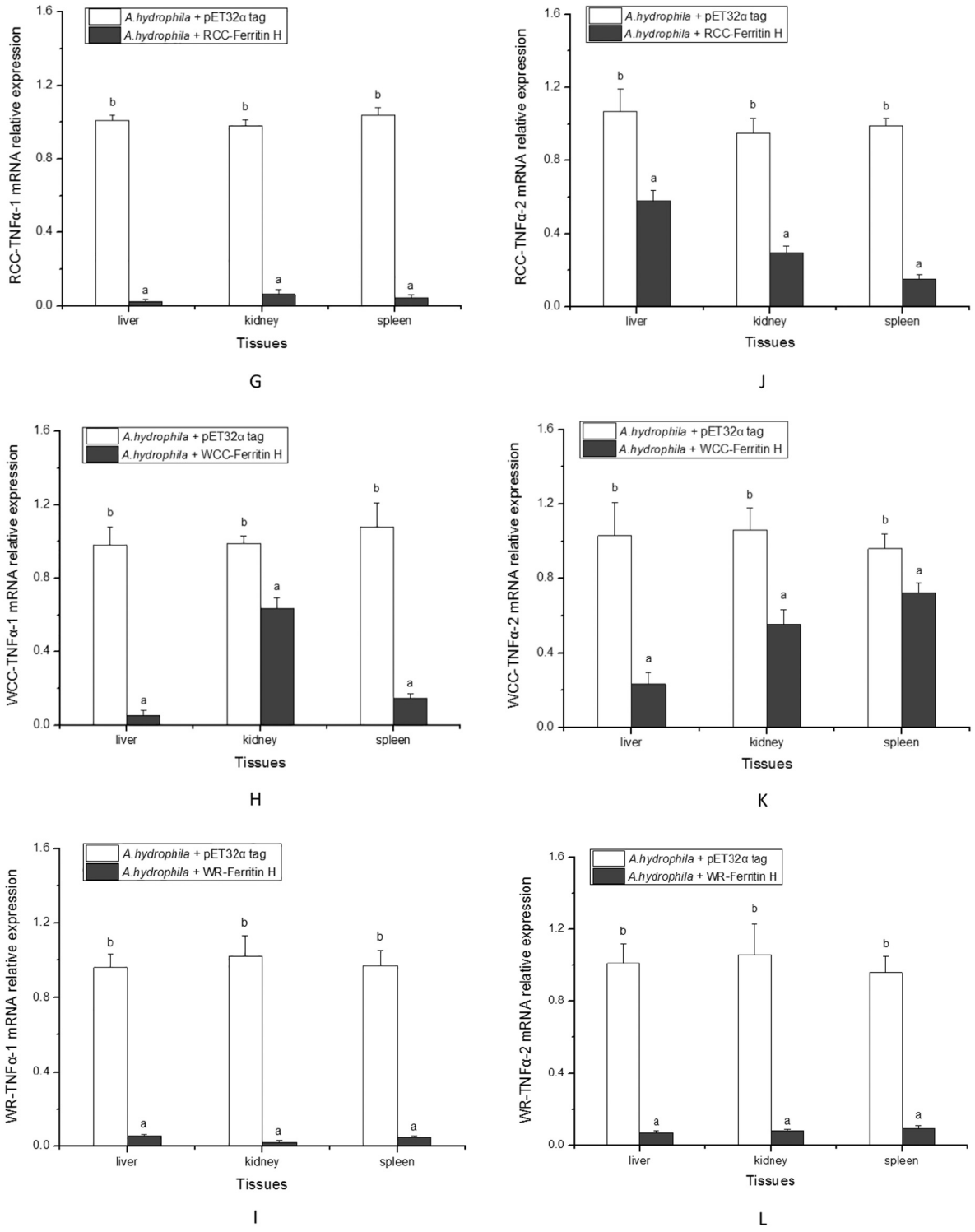

Fig. 7. (*continued*).

profiles of TIRAP, MyD88, TRAF6, IL-1β-1, IL-1β-2, TNFα-1 and TNFα-2 decreased dramatically in *A. hydrophila* + RCC/WCC/WR-Ferritin H group, suggesting that *in vivo* administration of RCC-Ferritin H, WCC-Ferritin H and WR-Ferritin H protein could attenuate *A. hydrophila*-induced inflammatory cascades and cytokine productions.

A. hydrophila infection and LPS stimulation can stimulate oxidative stress in fish (Chen et al., 2020; Luo et al., 2021c). Oxidative stress may refer to up-regulated level of intracellular ROS accumulation, then causing antioxidant imbalance and lipid peroxidation (Luo et al., 2015c; Schieber and Chandel, 2014). Additionally, fish liver contains abundantly various detoxification enzymes, playing a pivotal role in xenobiotic metabolism (Blom et al., 2000; Tao and Peng, 2009). As is well known, SOD and CAT are playing a critical role in the antioxidant defense against oxidative stress induced various stimuli, while MDA is mostly used as an end-product marker of lipid peroxidation during the occurrence of oxidative response (Farombi et al., 2007; Wei et al., 2010; Zhang et al., 2004). Current studies revealed that decreased MDA amounts and enhanced levels of total SOD and CAT activity in liver were

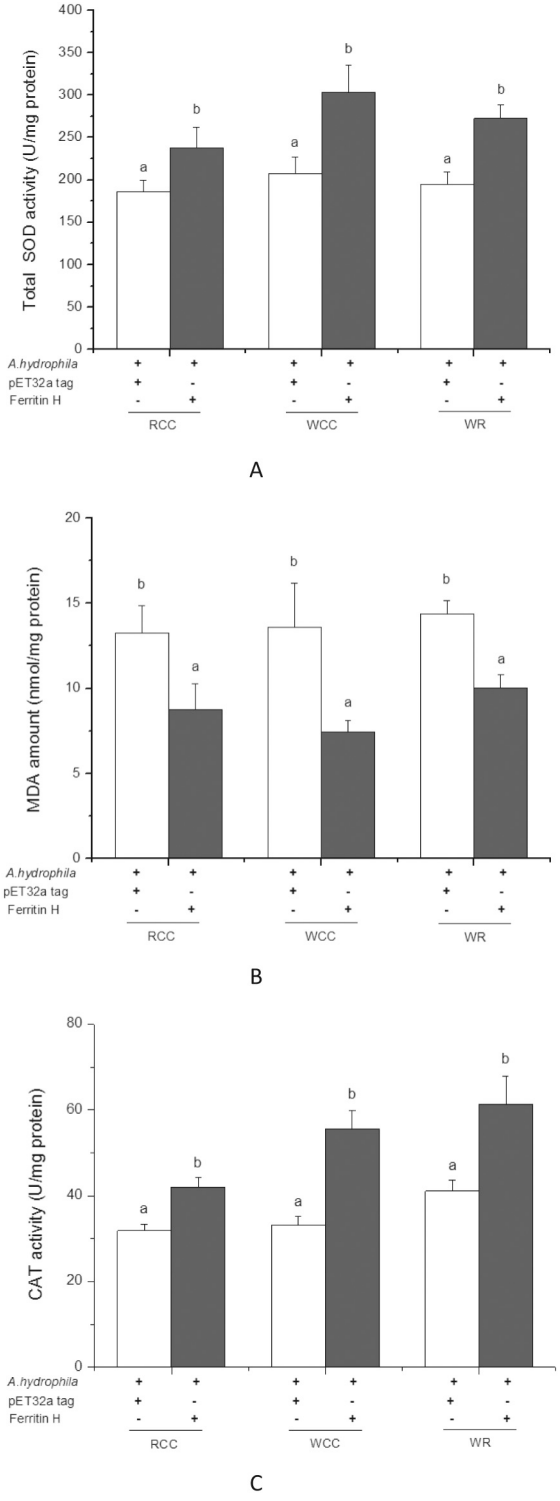

Fig. 8. *In vivo* administration of RCC-Ferritin H, WCC-Ferritin H and WR-Ferritin H fusion protein regulated antioxidant status. Liver total SOD activity (A), MDA amount (B) and CAT activity (C) were detected in RCCs, WCCs and WRs at 24 h post-challenge. The calculated data (mean ± SD) with different letters were significantly different ($P < 0.05$) among the groups. The experiments were performed in triplicate.

observed in *A. hydrophila* + RCC/WCC/WR-Ferritin H group. Although stress-induced iron release can trigger intracellular oxidative stress (Gilmour et al., 1997), Ferritin can protect cells from oxidant-mediated cytolysis *via* iron sequestrant (Balla et al., 1992). Moreover, overexpression of Ferritin H can reduce ROS accumulation in response to oxidant challenge (Orino et al., 2001). These results indicated that RCC-Ferritin H, WCC-Ferritin H and WR-Ferritin H could alleviate *A. hydrophila*-induced lipid peroxidation and maintain antioxidant activity. Thus, taken together, Ferritin H of hybrid offspring may elicit a similar suppression of *A. hydrophila*-induced inflammatory cascades and lipid peroxidation by comparing with those of its parents.

In summary, we compared tissue-specific expressions of RCC-Ferritin H, WCC-Ferritin H and WR-Ferritin H and studied their up-regulated expressions following *A. hydrophila* challenge. RCC-Ferritin H, WCC-Ferritin H and WR-Ferritin H fusion proteins could directly bind to *A. hydrophila* and LPS. *In vivo* administration of RCC-Ferritin H, WCC-Ferritin H and WR-Ferritin H fusion proteins could limit the *A. hydrophila* dissemination to tissues and lessen bacteria-induced inflammatory cascades and lipid peroxidation. Our results indicated that down-regulation of *A. hydrophila*-induced inflammatory signals by ferritin H were similar in hybrid fish and its parents.

Declaration of competing interest

The authors declare that they have no conflict of interest.

Acknowledgements

This research was supported by the National Natural Science Foundation of China, China (grant no. 31902363), Natural Science Foundation of Hunan Province, China (grant no. 2021JJ40340) and the Doctoral Publishing Fund of Hunan Normal University, China (grant no. 0531120-3680).

References

Andersen, O., Dehli, A., Standal, H., Giskegjerde, T., Karstensen, R., Rørvik, K., 1995. Two ferritin subunits of Atlantic salmon (Salmo salar): cloning of the liver cDNAs and antibody preparation. Mol. Mar. Biol. Biotechnol. 4, 164–170.

Andrews, N.C., 1999. Disorders of iron metabolism. N. Engl. J. Med. 341, 1986–1995.

Balla, G., Jacob, H.S., Balla, J., Rosenberg, M., Nath, K., Apple, F., Eaton, J., Vercellotti, G., 1992. Ferritin: a cytoprotective antioxidant strategem of endothelium. J. Biol. Chem. 267, 18148–18153.

Bayne, C.J., Gerwick, L., 2001. The acute phase response and innate immunity of fish. Dev. Comp. Immunol. 25, 725–743.

Beard, J.L., Murray-Kolb, L.E., Rosales, F.J., Solomons, N.W., Angelilli, M.L., 2006. Interpretation of serum ferritin concentrations as indicators of total-body iron stores in survey populations: the role of biomarkers for the acute phase response. Am. J. Clin. Nutr. 84, 1498–1505.

Blom, S., Andersson, T.B., Förlin, L., 2000. Effects of food deprivation and handling stress on head kidney 17a-hydroxyprogesterone 21-hydroxylase activity, plasma cortisol and the activities of liver detoxification enzymes in rainbow trout. Aquat. Toxicol. 48, 265–274.

Bowden, T.J., 2008. Modulation of the immune system of fish by their environment. Fish Shellfish Immunol. 25, 373–383.

Cha, G.-H., Luo, S.-W., Qi, Z.-H., Liu, Y., Wang, W.-N., 2015. Optimal conditions for expressing a complement component 3b functional fragment (a2-macroglobulin receptor) gene from Epinephelus coioides in Pichia pastoris. Protein Expr. Purif. 109, 23–28.

Chen, J., Liu, N., Zhang, H., Zhao, Y., Cao, X., 2020. The effects of Aeromonas hydrophila infection on oxidative stress, nonspecific immunity, autophagy, and apoptosis in the common carp. Dev. Comp. Immunol. 105, 103587.

Choo, G., Cho, H.-S., Park, K., Lee, J.-W., Kim, P., Oh, J.-E., 2018. Tissue-specific distribution and bioaccumulation potential of organophosphate flame retardants in crucian carp. Environ. Pollut. 239, 161–168.

Ding, Z., Zhao, X., Zhan, Q., Cui, L., Sun, Q., Wang, W., Liu, H., 2017. Comparative analysis of two ferritin subunits from blunt snout bream (Megalobrama amblycephala): characterization, expression, iron depriving and bacteriostatic activity. Fish Shellfish Immunol. 66, 411–422.

Diomede, F., Zingariello, M., Cavalcanti, M.F., Merciaro, I., Pizzicannella, J., de Isla, N., Caputi, S., Ballerini, P., Trubiani, O., 2017. MyD88/ERK/NFkB pathways and pro-inflammatory cytokines release in periodontal ligament stem cells stimulated by Porphyromonas gingivalis. Eur. J. Histochem. 61.

Farombi, E., Adelowo, O., Ajimoko, Y., 2007. Biomarkers of oxidative stress and heavy metal levels as indicators of environmental pollution in african cat fish (Clarias gariepinus) from Nigeria Ogun River. Int. J. Environ. Res. Public Health 4, 158–165.

Gilmour, P.S., Brown, D.M., Beswick, P.H., MacNee, W., Rahman, I., Donaldson, K., 1997. Free radical activity of industrial fibers: role of iron in oxidative stress and activation of transcription factors. Environ. Health Perspect. 105, 1313–1317.

Gonzalez-Serrano, C.J., Santos, J.A., Garcia-Lopez, M.L., Otero, A., 2010. Virulence markers in Aeromonas hydrophila and aeromonas veronii biovar sobria isolates from freshwater fish and from a diarrhoea case. J. Appl. Microbiol. 93, 414–419.
Holland, M.C.H., Lambris, J.D., 2002. The complement system in teleosts. Fish Shellfish Immunol. 12, 399–420.
Horng, T., Barton, G.M., Flavell, R.A., Medzhitov, R., 2002. The adaptor molecule TIRAP provides signalling specificity for toll-like receptors. Nature 420, 329–333.
Hunter, C.J., De Plaen, I.G., 2014. Inflammatory signaling in NEC: role of NFKB and cytokines. Pathophysiology 21, 55.
Karin, M., Lin, A., 2002. NF-?B at the crossroads of life and death. Nat. Immunol. 3, 221–227.
Kawai, T., Adachi, O., Ogawa, T., Takeda, K., Akira, S., 1999. Unresponsiveness of MyD88-deficient mice to endotoxin. Immunity 11, 115–122.
Koyama, H., Ito, T., Nakanishi, T., Sekimizu, K., 2007. Stimulation of RNA polymerase II transcript cleavage activity contributes to maintain transcriptional fidelity in yeast. Genes Cells 12, 547–559.
Li, Z., Wang, Z.W., Wang, Y., Gui, J.F., 2018. In: Crucian carp and gibel carp Culture. Aquaculture in China: Success Stories and Modern Trends, pp. 149–157.
Liu, B., Xu, L., Ge, X., Xie, J., Xu, P., Zhou, Q., Pan, L., Zhang, Y., 2013. Effects of mannan oligosaccharide on the physiological responses, HSP70 gene expression and disease resistance of allogynogenetic crucian carp (Carassius auratus gibelio) under Aeromonas hydrophila infection. Fish Shellfish Immunol. 34, 1395–1403.
Liu, H., Takano, T., Peatman, E., Abernathy, J., Wang, S., Sha, Z., Kucuktas, H., Xu, D.H., Klesius, P., Liu, Z., 2010. Molecular characterization and gene expression of the channel catfish ferritin H subunit after bacterial infection and iron treatment. J. Exp. Zool. A Ecol. Genet. Physiol. 313, 359–368.
Liu, Q., Liu, J., Liang, Q., Qi, Y., Tao, M., Zhang, C., Qin, Q., Zhao, R., Chen, B., Liu, S., 2019. A hybrid lineage derived from hybridization of Carassius cuvieri and Carassius auratus red var. and a new type of improved fish obtained by back-crossing. Aquaculture 505, 173–182.
Liu, Q., Qi, Y., Liang, Q., Xu, X., Hu, F., Wang, J., Xiao, J., Wang, S., Li, W., Tao, M., 2018. The chimeric genes in the hybrid lineage of Carassius auratus cuvieri (?)× Carassius auratus red var. (?). Sci. China Life Sci. 61, 1079–1089.
Liu, S., Luo, J., Chai, J., Ren, L., Zhou, Y., Huang, F., Liu, X., Chen, Y., Zhang, C., Tao, M., 2016. Genomic incompatibilities in the diploid and tetraploid offspring of the goldfish× common carp cross. Proc. Natl. Acad. Sci. 113, 1327–1332.
Livak, K.J., Schmittgen, T.D., 2001. Analysis of relative gene expression data using real-time quantitative PCR and the 2- ??CT method. Methods 25, 402–408.
Luo, J., Gao, Y., Ma, W., Bi, X., Wang, S., Wang, J., Wang, Y., Chai, J., Du, R., Wu, S., 2014a. Tempo and mode of recurrent polyploidization in the Carassius auratus species complex (Cypriniformes, Cyprinidae). Heredity 112, 415–427.
Luo, S.-W., Cai, L., Liu, Y., Wang, W.-N., 2014b. Functional analysis of a dietary recombinant fatty acid binding protein 10 (FABP10) on the Epinephelus coioides in response to acute low temperature challenge. Fish Shellfish Immunol. 36, 475–484.
Luo, S.-W., Cai, L., Qi, Z.-H., Wang, C., Liu, Y., Wang, W.-N., 2015a. Effects of a recombinant complement component C3b functional fragment a 2 MR (a 2-macro-globulin receptor) additive on the immune response of juvenile orange-spotted grouper (Epinephelus coioides) after the exposure to cold shock challenge. Fish Shellfish Immunol. 45, 346–356.
Luo, S.-W., Kang, H., Kong, J.-R., Xie, R.-C., Liu, Y., Wang, W.-N., Xie, F.-X., Wang, C., Sun, Z.-M., 2017. Molecular cloning, characterization and expression analysis of (B-cell lymphoma-2) Bcl-2 in the orange-spotted grouper (Epinephelus coioides). Dev. Comp. Immunol. 76, 150–162.
Luo, S.-W., Kang, H., Xie, R.-C., Wei, W., Liang, Q.-J., Liu, Y., Wang, W.-N., 2019a. N-terminal domain of EcC1INH in Epinephelus coioides can antagonize the LPS-stimulated inflammatory response. Fish Shellfish Immunol. 84, 8–19.
Luo, S.-W., Luo, K.-K., Liu, S.-J., 2020a. ITLN in diploid hybrid fish (Carassius auratus cuvieri?× Carassius auratus red var?) is involved in host defense against bacterial infection. Dev. Comp. Immunol. 103, 103520.
Luo, S.-W., Luo, K.-K., Liu, S.-J., 2020b. A novel LEAP-2 in diploid hybrid fish (Carassius auratus cuvieri?× Carassius auratus red var.?) confers protection against bacteria-stimulated inflammatory response. Comp. Biochem. Physiol., Part C: Toxicol. Pharmacol. 228:108665.
Luo, S.-W., Luo, Z.-Y., Yan, T., Luo, K.-K., Feng, P.-H., Liu, S.-J., 2020c. Antibacterial and immunoregulatory activity of a novel hepcidin homologue in diploid hybrid fish (Carassius auratus cuvieri?× Carassius auratus red var?). Fish Shellfish Immunol. 98, 551–563.
Luo, S.-W., Mao, Z.-W., Luo, Z.-Y., Xiong, N.-X., Luo, K.-K., Liu, S.-J., Yan, T., Ding, Y.-M., Zhao, R.-R., Wu, C., 2021a. Chimeric ferritin H in hybrid crucian carp exhibits a similar down-regulation in lipopolysaccharide-induced NF-?B inflammatory signal in comparison with Carassius cuvieri and Carassius auratus red var. Comp. Biochem. Physiol., Part C: Toxicol. Pharmacol. 241, 108966.
Luo, S.-W., Wang, W.-N., Cai, L., Qi, Z.-H., Wang, C., Liu, Y., Peng, C.-L., Chen, L.-B., 2015b. Effects of aDissostichus mawsoni-CaM recombinant proteins feed additive on the juvenile orange-spotted grouper (Epinephelus coioides) under the acute low temperature challenge. Fish Physiol. Biochem. 41, 1345–1358.
Luo, S.-W., Wang, W.-N., Sun, Z.-M., Xie, F.-X., Kong, J.-R., Liu, Y., Cheng, C.-H., 2016. Molecular cloning, characterization and expression analysis of (B-cell lymphoma-2 associated X protein) bax in the orange-spotted grouper (Epinephelus coioides) after the vibrio alginolyticus challenge. Dev. Comp. Immunol. 60, 66–79.
Luo, S.-W., Wei, W., Yang, P., Lai, C.-M., Liang, Q.-J., Liu, Y., Wang, W.-N., 2019b. Characterization of a CD59 in orange-spotted grouper (Epinephelus coioides). Fish Shellfish Immunol. 89, 486–497.
Luo, S.-W., Xiong, N.-X., Luo, Z.-Y., Fan, L.-F., Luo, K.-K., Mao, Z.-W., Liu, S.-J., Wu, C., Hu, F.-Z., Wang, S., 2021. A novel NK-lysin in hybrid crucian carp can exhibit cytotoxic activity in fish cells and confer protection against Aeromonas hydrophila infection in comparison with Carassius cuvieri and Carassius auratus red var. Fish Shellfish Immunol. 116, 1–11.
Luo, S.-W., Xiong, N.-X., Luo, Z.-Y., Luo, K.-K., Liu, S.-J., Wu, C., Wang, S., Wen, M., 2021c. Effect of lipopolysaccharide (LPS) stimulation on apoptotic process and oxidative stress in fibroblast cell of hybrid crucian carp compared with those of Carassius cuvieri and Carassius auratus red var. Comp. Biochem. Physiol., Part C: Toxicol. Pharmacol. 248, 109085.
Luo, S., Huang, Y., Xie, F., Huang, X., Liu, Y., Wang, W., Qin, Q., 2015c. Molecular cloning, characterization and expression analysis of PPAR gamma in the orange-spotted grouper (Epinephelus coioides) after the vibrio alginolyticus challenge. Fish Shellfish Immunol. 43, 310–324.
Luo, S.W., Wei, W., 2020. Molecular characterization of complement 9 in Epinephelus coioides and differential expression analysis of classical complement genes following Vibrio alginolyticus challenge. Ecotoxicology 29, 837–845.
Magnadottir, B., 2010. Immunological control of fish diseases. Mar. Biotechnol. 12, 361–379.
Marcogliese, D., 2008. The impact of climate change on the parasites and infectious diseases of aquatic animals. Rev. Sci. Tech. 27, 467–484.
Meneghini, R., 1997. Iron homeostasis, oxidative stress, and DNA damage. Free Radic. Biol. Med. 23, 783–792.
Muroi, M., Tanamoto, K.I., 2008. TRAF6 distinctively mediates MyD88-and IRAK-1-induced activation of NF-?B. J. Leukoc. Biol. 83, 702–707.
Ong, D.S.T., Wang, L., Zhu, Y., Ho, B., Ding, J., 2005. The response of ferritin to LPS and acute phase of pseudomonas infection. J. Endotoxin Res. 11, 267–280.
Orino, K., Lehman, L., Tsuji, Y., Ayaki, H., Torti, S.V., Torti, F.M., 2001. Ferritin and the response to oxidative stress. Biochem. J. 357, 241–247.
Papanikolaou, G., Pantopoulos, K., 2005. Iron metabolism and toxicity. Toxicol. Appl. Pharmacol. 202, 199–211.
Press, C.M., Evensen, Ø., 1999. The morphology of the immune system in teleost fishes. Fish Shellfish Immunol. 9, 309–318.
Qi, Z.-H., Liu, Y.-F., Luo, S.-W., Chen, C.-X., Liu, Y., Wang, W.-N., 2013. Molecular cloning, characterization and expression analysis of tumor suppressor protein p53 from orange-spotted grouper, Epinephelus coioides in response to temperature stress. Fish Shellfish Immunol. 35, 1466–1476.
Qi, Z., Zhang, Y., Chen, Z.-F., Yang, C., Song, Y., Liao, X., Li, W., Tsang, S.Y., Liu, G., Cai, Z., 2020. Chemical identity and cardiovascular toxicity of hydrophobic organic components in PM2. 5. Ecotoxicol. Environ. Saf. 201, 110827.
Rogers, R.L., Bedford, T., Hartl, D.L., 2009. Formation and longevity of chimeric and duplicate genes in Drosophila melanogaster. Genetics 181, 313–322.
Schieber, M., Chandel, N.S., 2014. ROS function in redox signaling and oxidative stress. Curr. Biol. 24, R453–R462.
Schmedes, A., Hølmer, G., 1989. A new thiobarbituric acid (TBA) method for determining free malondialdehyde (MDA) and hydroperoxides selectively as a measure of lipid peroxidation. J. Am. Oil Chem. Soc. 66, 813–817.
Scudiero, R., Esposito, M.G., Trinchella, F., 2013. Middle ferritin genes from the icefish Chionodraco rastrospinosus: comparative analysis and evolution of fish ferritins. C. R. Biol. 336, 134–141.
Šimková, A., Dávidová, M., Papoušek, I., Vetešník, L., 2013. Does interspecies hybridization affect the host specificity of parasites in cyprinid fish? Parasit. Vectors 6, 95.
Šimková, A., Vojtek, L., Halacka, K., Hyršl, P., Vetešník, L., 2015. The effect of hybridization on fish physiology, immunity and blood biochemistry: a case study in hybridizing Cyprinus Carpio and Carassius gibelio (Cyprinidae). Aquaculture 435, 381–389.
Tao, T., Peng, J., 2009. Liver development in zebrafish (Danio rerio). J. Genet. Genomics 36, 325–334.
Triantafilou, M., Brandenburg, K., Kusumoto, S., Fukase, K., Mackie, A.R., Seydel, U., Triantafilou, K., 2004. Combinational clustering of receptors following stimulation by bacterial products determines lipopolysaccharide responses. Biochem. J. 381, 527–536.
Van Doan, H., Doolgindachabaporn, S., Suksri, A., 2013. The LD50 of Asian Catfish (Pangasius bocourti, Sauvage 1870) challenge to pathogen Aeromonas hydrophila FW52 strain. In: Pensee, p. 75.
Wang, C.-Y., Mayo, M.W., Baldwin, A.S., 1996. TNF-and cancer therapy-induced apoptosis: potentiation by inhibition of NF-?B. Science 274, 784–787.
Wang, J., Xiao, J., Zeng, M., Xu, K., Tao, M., Zhang, C., Duan, W., Liu, W., Luo, K., Liu, Y., 2015. Genomic variation in the hybrids of white crucian carp and red crucian carp: evidence from ribosomal DNA. Sci. China Life Sci. 58, 590–601.
Wang, L., Fan, C., Xu, W., Zhang, Y., Dong, Z., Xiang, J., Chen, S., 2017. Characterization and functional analysis of a novel C1q-domain-containing protein in japanese flounder (Paralichthys olivaceus). Dev. Comp. Immunol. 67, 322–332.
Wei, D., Zhang, X.L., Wang, Y.Z., Yang, C.X., Chen, G., 2010. Lipid peroxidation levels, total oxidant status and superoxide dismutase in serum, saliva and gingival crevicular fluid in chronic periodontitis patients before and after periodontal therapy. Aust. Dent. J. 55, 70–78.
Worwood, M., 1990. Ferritin. Blood Rev. 4, 259–269.
Yu, M., Li, S.-M., Li, X.-Y., Zhang, B.-J., Wang, J.-J., 2008. Acute effects of 1-octyl-3-methylimidazolium bromide ionic liquid on the antioxidant enzyme system of mouse liver. Ecotoxicol. Environ. Saf. 71, 903–908.

Zandman-Goddard, G., Shoenfeld, Y., 2007. Ferritin in autoimmune diseases. Autoimmun. Rev. 6, 457–463.
Zhang, J., Shen, H., Wang, X., Wu, J., Xue, Y., 2004. Effects of chronic exposure of 2, 4-dichlorophenol on the antioxidant system in liver of freshwater fish Carassius auratus. Chemosphere 55, 167–174.
Zhang, X., Wei, W., Wu, H., Xu, H., Chang, K., Zhang, Y., 2010. Gene cloning and characterization of ferritin H and M subunits from large yellow croaker (Pseudosciaena crocea). Fish Shellfish Immunol. 28, 735–742.
Zhu, B.-S., Xing, C.-G., Lin, F., Fan, X.-Q., Zhao, K., Qin, Z.-H., 2011. Blocking NF-KB nuclear translocation leads to p53-related autophagy activation and cell apoptosis. World J. Gastroenterol. 17, 478–487.